Section A-Research Paper
ISSN 2063-5346

CFD ANALYSIS OF EARTH TEMPERATURES UNDER A VARIETY OF SOIL-SURFACE CONDITIONS WITH EXPERIMENTAL VALIDATION

Gajendra Kumar*, Radha Krishna Prasad, and Ram Vinoy Sharma
Department of Mechanical Engineering, NIT Jamshedpur, Jharkhand, INDIA, 831014
Corresponding Author*: 2015rsme003@nitjsr.ac.in

Article History: Received: 11.04.2022 Revised: 18.05.2022 Accepted: 11.06.2022

DOI:10.53555/ecb/2022.11.6.134

Nomenclature

K : Thermal conductivity [$W.m^{-1}.K^{-1}$]
CE : Convective energy [W]
LR : Long wave emissive radiation [$W.m^{-2}$]
SR : Soil radiation [$W.m^{-2}$]
LE : Latent heat flux due to evaporation [$W.m^{-2}$]
h_s : Total transmission of heat coefficient for soil surface [$W.m^{-2}.K^{-1}$]
FDM : Finite difference method
T : Earth Temperature [K] T_e : Effective temperature [K] t : Time [s]
y : Depth from earth surface [m] α : Thermal diffusivity [$m^2.S^{-1}$] yearly depth wise soil temperature. The amplitude of soil temperature fluctuations is found to be up to 0.2 m depth for daily fluctuation in all mentioned surface conditions, while for annual fluctuation, it reaches up to 4 m depth. The depth-wise soil temperature achieves its lowest value for wet sheltered surface condition for both daily and yearly fluctuations, whereas the highest value is achieved for sunlit soil surface condition.

ABSTRACT
The objective of this study is to analyze the temperature of soil at various depths, taking into account different surface conditions, including dry and wet surfaces under sunlit and sheltered conditions, subject to time- varying boundary conditions. The mathematical approach used to evaluate soil temperature involves the Fourier method, which employs six harmonic terms of atmospheric temperature of air and earth- surface radiation from sun. The software ANSYS 19.0 Fluent is utilized to compare the mathematical Fourier results for transient boundary conditions for daily and

Keywords: Thermal behavior of Soil, Fourier analysis, CFD.

ρ	:	Density of soil [Kg.m^{-3}]
Ψ	:	Phase difference
ω	:	2Π/time [rad. s^{-1}]

Subscript

0	:	First term of Fourier series
m	:	Number of terms
e	:	Effective
a	:	Ambient
h_c	:	Transmission of heat due to convection coefficient [W.m^{-2}. K^{-1}]
h_r	:	Radiative transmission of heat coefficient [W.m^{-2}. K^{-1}]
h_e	:	Effective transmission of heat coefficient [W.m^{-2}. K^{-1}]
ε	:	Emittance of earth surface
v	:	Velocity of air [m.s^{-1}]
σ	:	Stefens Boltzmann constant [W.m^{-2}. K^{-4}]
$\dot{m}_e$	:	Soil surface mass evaporation [Kg. s^{-1}]
L	:	Latent heat of vaporization [KJ. Kg^{-1}]
P_S	:	Saturated water vapor pressure [Pa]
γ	:	Relative humidity
f	:	Evaporation rate coefficient
α_0	:	Soil surface absorptivity
c_p	:	Specific heat capacity [KJ. Kg^{-1}. K^{-1}]

1.0 Introduction

Thermal properties play a crucial role in energy storage, and soil has been used for this purpose for a long time, such as in earth air heat exchangers and agricultural applications. Soil temperature significantly impacts biological processes in agriculture, such as seed germination, seed growth, and root formation. Soil temperature is influenced by various parameters, including height above sea level, humidity, atmospheric conditions, soil properties, water content in the soil, and rainfall in the area. The environmental factors taken into consideration in this study include atmospheric conditions that include surrounding temperature of air, humidity, and radiation from sun that vary seasonally, making it challenging for researchers to measure soil temperature daily and throughout the year at different depths.

Radiation from sun data and ambient temperature of air are easily measurable parameters in space that directly impact changes in temperature on the soil surface and below it. Predicting soil temperature at different depths and times requires these parameters.

Previous research has shown that soil temperature fluctuations caused by climate change are complicated. Among all relationships, commonly acknowledged connection stands out. According to this correlation, the earth temperature fluctuates sinusoidally with depth over time [1]. The rate of change in earth temperature steadily reduces as depth increases until it achieves a stable state. Numerous investigations [2-6] have been conducted on the energy balance of the Earth's surface. A correlation is established between radiation from sun and the ambient Earth's temperature as a function of time and depth [2]. The energy balance equation was applied in Kuwait to analyze the daily and yearly changes in earth temperature. On the earth's surface, energy balance is employed as

a condition of the boundary to investigate the effect of land on surface temperature [3]. The impact of different surface conditions, such as bare soil, short and tall grass, a forest, and two agricultural crops, was evaluated [4]. The study of thermal engagement between a building and the earth revealed that the primary method for determining the normal temperature of the earth at a particular depth and season is to utilize simple semi- empirical formulae using data from the earth's surface at a specific place [5]. However, because of the absence of earth surface temperature information in the atmospheric records, this method is not universally applicable. Regardless of the data's availability, there are three different parameters in this category that use energy balance as the earth surface boundary condition. The earth surface boundary condition is composed of three parameter:

radiation from sun, cold sky's heat loss via long-wavelength radiation from sun, and transfer of heat due to convection between the surrounding atmosphere and the earth surface [6]. Different models have been presented to measure soil temperature fluctuations. A sinusoidal harmonic model was used to analyze the heat transmission in an exposed concrete block when the earth surface was subjected to a heat flux that included radiation from sun and convection as boundary conditions [7]. Similarly, Using the harmonic fluctuation in worldwide radiation from sun and ambient temperature, a model was developed for analyzing soil temperature [8].

It is generally agreed that numerical models are more trustworthy and accurate when used to analyze different soil typologies and boundary conditions. Numerical approaches, on the other hand, take more time to implement and solve the issue [9]. At the soil surface level, constant surface temperatures or heat fluxes are frequently used as boundary conditions. Numerical approaches, on the other hand, take more time to implement and solve the issue. In studies of soil thermal behavior, it is common to use either constant surface temperatures or heat fluxes as boundary conditions at the earth surface level [7]. However, determining the temperature of soil surface can be a challenge since typical meteorological stations do not track this characteristic. To overcome this issue, researchers may sometimes approximate the temperature of soil surface to be similar to the surrounding temperature of air [10]. Nonetheless, computational investigations that consider the relationship between soil and the surroundings, involving heat and moisture transmission, and can simulate periodic boundary conditions tend to yield more accurate results than analytical models. In fact, it has been shown that analytical techniques for predicting soil temperature frequently fail. The researchers made a comparison between two different models to investigate their applicability in predicting soil thermal behavior. One of the models involved a harmonic

approach that utilized surface heat flow as a boundary condition, while the other model utilized the finite difference method (FDM) as a numerical technique for solving soil transmission of heat equations. By evaluating and contrasting the results obtained from both models, the researchers aimed to identify which one would be more effective and accurate in forecasting soil temperature changes. Even though this computational model makes it possible to estimate short-term fluctuations, it hasn't been supported by experimental data [11].

One-dimensional model of soil using the finite difference method has been used for predicting the soil temperature. The finite difference method is used to discretize the one-dimensional transient heat conduction equation, and experimental data is used to verify the outcomes [12]. Computer technique has been created that can predict changes in soil temperature quantitatively which included heat and moisture transport processes that needed inputs like soil irrigation or precipitation [13]. FDM can predict daily changes in temperature at the hourly level, but it requires several input parameters and does not have experimental validation. The model was also used in a numerical analysis to calculate soil temperature [14]. To increase accuracy, they took into account evaporation in addition to heat diffusion, convection, and radiation. They included a method in their model for calculating soil water content, which varies with rainfall rate, also developed a model for thermal capacitance and conductivity, which vary according to the soil's moisture content. The temperature of the soil at depths where seasonal changes have no effect is referred to as the "undisturbed earth temperature". The most accurate way to establish that these temperature values vary depending on location is to conduct deep- earth experimental observations. Because such experimental observations may be challenging to make in real-world circumstances, the value of undisturbed temperature may be calculated using a variety of techniques. The most straightforward is to assume that the temperature of the undisturbed earth is the same as the yearly average temperature of air. This presumption might not be true in climates with a high degree of variability [15]. As a result, using the average soil surface temperature may provide greater precision than using the average temperature of air. It is challenging to calculate the average soil surface temperature because traditional weather stations rarely measure this parameter. Numerous other methods of simulating soil temperature have been developed, including numerical methods, analytical and semi- empirical methods [16], and purely empirical methods [17]. Due to difficulties in precisely determining the earth surface boundary conditions and the actual thermal properties of the soil [18].A significant portion of these analytical and numerical approaches may not always produce accurate and current forecasts of earth temperature fluctuation. Air and solar intensity data are evaluated and measured and soil temperature fluctuation are measured applying one-dimensional governing heat conduction equation with the

appropriate boundary conditions for four different soil conditions in Delhi (India) using the Fourier equation [18]. On short- grass surfaces, experimental validation was compared to the ANN technique and numerical analysis [19]. After examining six climatic zones across the United States, a linear regression method was used to predict soil temperature [17], [20]. To ascertain the affiliation between changing temperature of soil and changing temperature of air as precisely as possible, experiments are required [21]. The finite difference method was used to numerically model a dry, sunny scenario for prediction of soil temperature [22].

is sheltered, exposed to direct sunlight, or both, affect the soil's temperature. In this literature, soil temperature variations for different soil surface conditions, including dry sunlit, wet sunlit, dry sheltered, and wet sheltered, have been analyzed using CFD for Jamshedpur (India) region.

For numerical modeling of soil temperature measurement, the majority of researchers [7, 15, and 18] have used the average temperature of air as a boundary condition on the surface of earth. However, in this study, the average soil surface temperature is used as a boundary condition to achieve better accuracy. The average temperature of soil surface is

$$\frac{\partial^2}{} \quad -\frac{\partial\ (y,t)}{} \qquad (1)$$

Where α denotes soil thermal diffusivity and y denotes depth fluctuation below the earth surface. At the earth's surface, a numerical solution to the above equation can be found using the suitable boundary condition equation[24].

$$-K\_\frac{\partial T}{\partial y}\Big|_{y=0} = CE - LR + SR - LE \quad (2)$$

$$\frac{T(y,t)}{t} = -\frac{1}{\partial^2} \frac{T}{\partial} \qquad y \qquad \alpha$$

various depths and times. Because of the energy balance equation's integrated effects of convective energy exchange between air and soil surfaces, Long wavelength radiation released by the earth's surface, sunlight absorbed by the earth's surface, and evaporative latent heat flow, it is possible to measure the effective temperature using experimentally measured temperature of air, speed of wind, and radiation from sun. The soil's surface conditions, such as whether it difficult to measure with accuracy. The computer program ANSYS 19.0 Fluent (CFD), which uses the energy balance as a boundary condition on the soil surface to precisely measure the fluctuation in temperature of soil, is used in this study to investigate the thermal behavior of soil at the earth surface) over both annual and daily cycles.

The one-dimensional, transient heat conduction equation [23] was utilized in order to represent the change in soil temperature T (y, t).

2.0 Fourier Analysis

A complex function can be broken down mathematically into a number of simpler sinusoidal functions using the Fourier analysis method. Any periodic function can be expressed using Fourier

analysis as the sum of sine and cosine waves with various amplitudes, phases, and frequencies. Partial differential equations involving time and space variables can also be solved using Fourier analysis. In order to analyze non- periodic functions or signals, the Fourier transform is a Fourier analysis extension. The earth is typically modeled as a finite- thickness plate in numerical calculations, with periodic fluctuations in heat fluxes occurring on the earth's upper surface (i.e., Here, CE is the symbol for convective energy exchange, which occurs between the air and the surface of the soil., while thermal conductivity is represented by K, Long wave radiation, radiation from sun, and latent heat flux by evaporation are represented by LR, SR, and LE.

Convective Energy (CE): Convective energy refers to the energy transfer that occurs due to the movement of fluids, such as gases and liquids, caused by temperature differences or other external forces. This type of energy transfer involves the transfer of both heat and mass, and it is an important mechanism for transmission of heat in many natural and engineered systems.

Based on the transmission of heat between the soil surface and the air, this equation calculates convective energy (CE) [23].

$$CE = ⍰_s\,(T_a - T\,|_{y=0}) \qquad (3)$$

Here, $T|_{y=0}$ is the soil surface temperature, T_a is the temperature of air, and h_s is the soil surface transmission of heat due to convection coefficient.

Soil radiation (SR): Electromagnetic radiation is a form of energy that can either be released or absorbed by soil surfaces. It is essential for maintaining the energy balance of the Earth's surface and for a wide variety of natural and agricultural systems to transfer radiation between the soil surface and the surrounding environment. A radiation from sun analysis equation can be used to determine how much radiation from sun the earth surface absorbs.

$$SR = \alpha_0.\, S(t) \qquad (4)$$

Here α_0 is the soil radiation absorptivity at the earth surface and S(t) is the intensity of radiation from sun given in terms of the Fourier transform.

Long wave emissive radiation (LR): It refers to the thermal radiation emitted by objects with a temperature above absolute zero in the form of electromagnetic waves radiation emitted by a soil surface exposed to the sky and surroundings.

$$⍰_r = 4\varepsilon\sigma(T_a + 273.15)^3 \qquad (9)$$

The sky temperature, T_{sky} is approximated as,

The computation of the variables h_s and ΔR in equations (3) and (5) follows the method described by Kays and Crawford [25]. In this context, h_s represents the total transmission of heat coefficient, which takes into account both

convective and radiative transmission of heat coefficients. The convective term is influenced by the velocity of the air, while the radiative term is influenced by the temperature of the air.

$$\text{□}_s = \text{□}_c + \text{□}_r \quad (7)$$

On the soil surface, long wave radiation is consistent and can be represented by the following:

$$LR = \varepsilon . \Delta R \quad (5)$$

$$\Delta R = \sigma\,(T_a + 273.15)^4 - (T_{sky} + 273.154 \quad (6)$$

Here, ε refers to the emittance of the earth surface, while as a function of temperature;
ΔR is the difference between the radiation emitted by a black substance at the surrounding temperature of air and the $T_{sky} = (T_a + 273.15) - 12$ (10)

Latent heat flux due to evaporation (LE): It is the amount of heat needed to change the state of water from liquid to gas without altering its temperature, is transferred from the soil's surface to the atmosphere as water evaporates. This transfer of energy is referred to as LE, or the energy transferred from the Earth's surface to the atmosphere.

The equation can be applied in order to determine the latent transmission of heat that is caused by evaporation from the surface of the earth.

$$LE = \dot{m}_e L \quad (11)$$

This relation holds true for the transmission of heat due to convection coefficient of a surface that is subjected to the ambient air speed (v):

$$\text{□}_c = 2.8 + 3v \quad (8)$$

The expression for the long wave radiation, ΔR, can be given as:

Here, $\dot{m}_e$ denotes the rate of soil surface mass evaporation and L is latent heat of evaporation.

The amount of water evaporating from the surface of the soil is determined by the following equation [25].

$$\dot{m}_e L = 0.0168 f \text{□}_s [Ps(T|_{y-0}) - \quad (12)$$

$$\gamma PsTa$$

This equation involves the saturated water vapor pressure (P_S) and the relative humidity (γ).

$$Ps = R_1 T + R_2 \quad (13)$$

In the P_S expansion, R_1=103 Pa K^{-1} and R_2=609 Pa are constants.

The fraction f can be calculated using the formula Penman [26]

a) For bare soils, f varies according to the

$$\frac{\partial}{\partial} \_ k\, y^T \Big|_{y=0} = \text{□}_e (T_e - T|_{y=0}) \quad (15)$$

Here, $\square_e = \square_s(1 + 0.0168fR_1)$ (16) and,

$$T = {}^{1}[\square\ (1 + 0.0168fR\ \gamma)T +$$

e $\square_e$ s 1 a

$$\alpha 0S(t) - \varepsilon\Delta R - 0.0168fR2\square s\ (1-\gamma)$$

(17)

moisture content of the soil. For example, f = 1 represents saturated soils, f= 0.6-0.8 represents wet soils, f= 0.4-0.5 represents moist soils, and f= 0.1-0.2 represents arid soils. Because there is no moisture loss in dry soils, f= 0[27].

b) For covered soils, the fraction f is calculated by multiplying 0.70 by the αmy (19)

value of f calculated in step (a) based on soil moisture content [28].

Putting the above equation together (3), (4), (5), and (11) in equation (2) produce

$$\frac{\partial}{\partial}\ \_k\ T\Big|_{y\ y=0}^{s} = \square \quad (T_a - T|_{y=0}) - \varepsilon\Delta R + m^{1/2}\mu) + m\mu^2$$

$$\alpha^0 S(t) - \mathrm{m}\cdot_e L \qquad (14)$$

Equations (12) and (13) in (14) can be written as follows:

In general, the periodic function T_e is able to be represented as an annual and daily Fourier series.

$$T_e = T_0 + \sum_{m=1}^{\infty} T_m \cos\square(m\omega t - \psi_m)$$

(18)

The solution to the equation for heat conduction in one dimension may be stated as follows (with the assumption that T is finite for y→∞) is expressed as follows:

$$T\ t_m \quad (y,t) = t_0 + \sum_{m=1}^{\infty} \exp\square[i(m\omega t) +$$

Here,

$\alpha_m = -(1 - i)(\omega\sigma\mathrm{cm}/2k)^{1/2}$ (20) After substituting T_e and T(y, t) using equations (18) and (19) into equation (15), some algebraic manipulation leads to the following result.

$$T = T_0 + \sum B_m \exp\square(-m^{1/2}\alpha y)\cos\square(\ m\omega t$$

Here,

$$m^{1/2}\alpha y - \psi m - \beta m \quad (21)$$

$$B_m = T_m\,(1 +$$

(22)

$$\mu = (\ \frac{k\omega\sigma c}{2}\ )^{\frac{1}{2}}\ /\square_s \qquad (23)$$

$$\beta_m = \tan^{-1}\left[\frac{m^{1/2}\mu}{(1+m^{1/2}\mu)}\right] \quad (24)$$

Because the equation used before is for annual fluctuation, the equation for daily fluctuation is as follows:

$$T_{daily} = T_{ammual-avg} + \sum B_m \exp(-m^{1/2}\alpha y)\cos(m\omega t - m^{1/2}\alpha y - \psi m - \beta m) \quad (25)$$

3.0 Experimental Analysis

An experimental setup was installed on the campus of the National Institute of Technology in Jamshedpur, Jharkhand (Latitude 22^0 46' 40.51^0 N, Longitude 86^0 8' 33.08'E and Altitude 167m above mean sea level) to accurately measure soil temperature variation. The setup comprises of a 3-meter-long PVC pipe with a diameter of 25mm, on which eight thermocouple sensors (RTD PT-100) are mounted. These sensors are positioned at various depths of 0.1m, 0.2m 0.3m, 0.4m, 0.5m, 1m, 2m, and 3m ranging from earth surface (0m) to 3m, connected to a temperature data logger. Temperature readings are recorded at one minute interval for entire year 2021. By drilling a hole that is 3 m long and 100 mm in diameter, the PVC pipe with the sensors attached is placed into the ground. The mounted temperature sensors are attached to the PVC so that they are perpendicular to the pipe and outside of it, and when they are installed in the borehole, they come into direct contact with the soil. To guarantee a tight fit, the soil excavated during hole- digging is used to fill the space between the PVC pipe and the ground.The

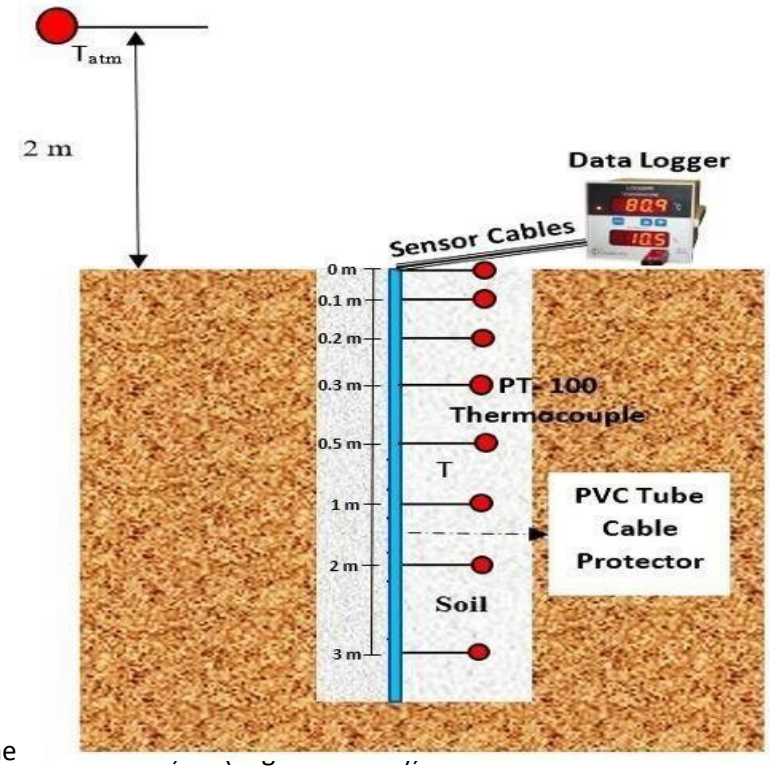

Figure 1. A schematic diagram depicting the experimental arrangement for measuring the in-earth temperatures (T) at various depths and the ambient temperature of air (T_{atm})

ISSN 2063-5346

experimental arrangement for measuring the in-earth temperatures at various depths and the ambient temperature of air is depicted in Figure 1.

Soils which are removed during drilling mainly consist of red soil. For measuring the soil properties with SH-1 probe soil in the shape of cube of same size of SH-1 probe measuring container is removed by drilling so the compactness of soil is maintained. The soil removed in the hot summer day is mainly consisting of dry soil with negligible water content up to depth of 0.5 m. The amount of water content in the soil at depth of 1m, 2m, and 3m consist of 20 % irrespective of the season. The amount of water in soil is determined by the difference between the mass of soil that is removed from the earth during drilling and the mass of soil that is dried by sunlight. During cold winter day soil removed from the earth by drilling consist of water content of 20% throughout the depth. These properties are measured using a constant thermal analyzer with an SH-1 probe, as depicted in Figure 2(a). Table 1 and Table 2 present the physical properties of dry soil and soil with a water content of 20%, respectively.

Table 2. Wet soil surface Properties (20% of water content)

S.no.	Parameter	Symbol	Value	Unit
1.	Thermal conductivity of Soil	K	1.19	W/m K
2.	Density of soil	ρ	2029.80	Kg/m^3
3.	Specific heat capacity of soil	c_p	756.108	J/kg K
4.	Soil surface absorptivity	α_0	0.65	-
5.	Emittance of earth surface	ε	0.8	-
6.	Relative humidity of soil	ϒ	0.04	-

Table 1. Dry soil surface Properties

S.no.	Parameter	Symbol	Value	Unit
1.	Thermal conductivity of Soil	K	0.5642	W/m K
2.	Density of soil	ρ	1968	Kg/m^3
3.	Specific heat capacity of soil	c_p	941.86	J/kg K

Radiation from sun, speed of wind, and ambient temperature of air data were collected using a solar radiation and meteorological parameter device placed at the National Institute of Technology in Jamshedpur, as shown in Figure 2(b). About 50 m apart from a solar radiation and meteorological parameter device, an experimental setup was installed to measure soil temperature. The data was recorded every minute for the entire year and can be accessed online on the CWET website, managed by the Ministry of New and Renewable Energy (MNRE), Government of India. The ambient temperature of air data was represented in the form of a Fourier series, and the daily mean average temperature was calculated. The highest daily mean

average temperature for the year 2021 was observed on 17th June during the summer season, while the lowest daily mean average temperature for the same year was recorded on 28th December during the winter season.

(a) (b)

Figure 2 (a) Measurement of thermal conductivity and diffusivity of soil by thermal analyzer and (b) Measurement of Meteorological Parameters at CWET station, NIT Jamshedpur

4.0 CFD Analysis

Computational Fluid Dynamics (CFD) is a powerful tool for analyzing heat and mass transfer problems. It involves solving the governing equations of mass, momentum, and energy at discrete grid points or cells of the system. CFD software applies these equations to each grid point to obtain the temperature distribution, pressure fluctuation, flow pattern, and other relevant parameters in a short period of time and with reduced costs compared to experimental work. The convergence technique used in CFD ensures that the solution is accurate and reliable. By using CFD, engineers and scientists can optimize the design of systems, predict their behavior under different conditions, and improve their efficiency and performance.

In ANSYS Workbench, a two-dimensional geometry with axis-symmetry, measuring 10 meters in depth and 1 meter in width, has been constructed to analyze the temperature changes in a soil system through CFD simulations. This

ISSN 2063-5346

geometry is illustrated in Figure 3. In order to obtain information on temperature distribution and simulate transmission of heat in the soil system, this design is used. The dimensions and material characteristics of the rectangular block accurately represent the soil system. To simulate the transmission of heat within the soil system, the CFD software will apply the governing equations to each cell of the rectangular block. A range of environmental conditions, including the ambient temperature of air, radiation from sun, and speed of wind, can be used to conduct the simulation and forecast temperature distribution in the soil system. The outcomes can be used to enhance the performance of the soil system and optimize its design.

The grid sensitivity test is an important step in CFD modeling to ensure that the numerical solution is not affected by the grid resolution. In this test, the soil temperature is simulated for different grid sizes, and the results are compared to determine the optimum grid size beyond which the soil temperature remains constant. The grid optimization test is shown in Figure 4.

This indicates that the mesh is sufficiently refined and that adding more elements won't significantly increase the accuracy of the outcomes. A transient

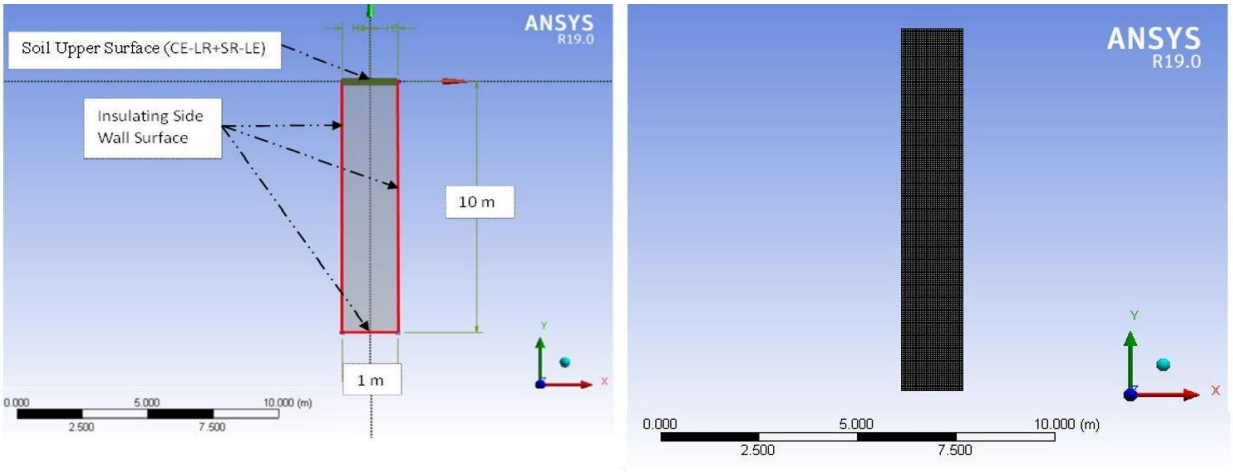

(a) (b)

Figure 3. Geometry(a) and meshing(b) of modal

For the given geometrical model, ANSYS 19.0 Fluent has produced a structural mesh with an equal distribution of grid. The grid density of the elements was examined from 100,000 to 1,200,000, and it was discovered that after 520,000 elements, the sensitivity quantity, in this case the surface temperature, becomes constant.

analysis is used to simulate the seasonal and daily fluctuation of soil temperature. The upper surface of the soil is assumed to have convective boundary conditions, whereas the other three sides of the soil are treated as insulated. For convective boundary condition, user-defined Fourier equation is used to apply the atmospheric temperature as T_e and transmission of heat coefficient is taken as h_e to all four soil surface conditions in order to simulate the yearly fluctuation

of soil temperature. Similar to this, T_e and h_e of daily fluctuation is used to account for daily fluctuation soil temperature analysis using a user-defined Fourier equation with six terms as shown in Tables 5, 6 and 7. Four surface conditions are dry sunlit surface, dry sheltered surface, wet sunlit surface, and wet sheltered surface. Dry represent the soil which is having no water content and wet represent the soil with water content of 20 %. Sunlit surface receive the direct sunlight radiation while sheltered surface don't receive direct sunlight. The time-varying nature of the boundary conditions is taken into account by the transient analysis, which also provides information on temperature distribution at each time step. A time step of 300 seconds is taken in the simulation for yearly fluctuation and time step of 60 seconds is taken for daily fluctuation under all soil surface conditions. The analysis of the soil system's internal transmission of heat and design optimization for enhanced performance can be done using this data. The SIMPLE algorithm is used for the simulation process, with the second upwind condition, and the convergence criteria are set to 10^{-6}. By first applying the yearly fluctuation up to the day before the given hottest and coldest day, and then setting the atmospheric temperature of a daily Fourier series for the appropriate soil surface conditions, the hottest summer day and the coldest winter day are simulated for daily fluctuation. The initial soil temperature is used throughout the process as the T_0 value of the yearly undistributed soil temperature. These simulations are run to obtain the temperature distribution at each time step and to examine the behavior of the soil system under various scenarios. Soil-based energy systems can be designed and optimized with the help of this information.

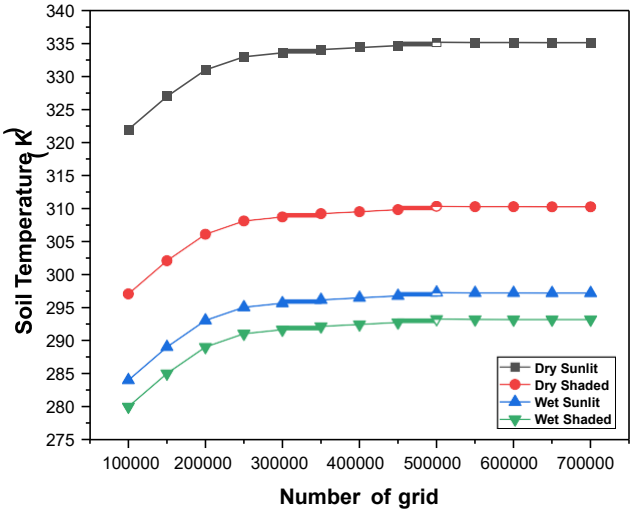

Figure 4. Grid sensitivity test

Section A-Research Paper
ISSN 2063-5346

5.0 Result and discussion

For the Jamshedpur (India) location, the distribution of temperatures in the soil is determined by temperature of air and radiation from sun, which may be described as a six- term Fourier series.

Table 3. Fourier series of temperature of air in Jamshedpur.

		0	1	2	3	4	5	6
yearly	T_0	26.33						
	Constant COS term		-4.84	-2.39	-0.44	-0.46	0.45	-0.50
	Constant SIN term		0.32	-0.93	0.30	-0.83	-0.16	-0.13
hottest	T_0	36.55						
	Constant COS term		-3.17	-0.33	-0.28	-0.04	0.27	-0.04
	Constant SIN term		-4.69	0.72	0.03	-0.10	-0.21	-0.16
coldest	T_0	19.5						
	Constant COS term		-1.69	0.34	-0.31	0.18	-0.04	-0.04
	Constant SIN term		-2.39	0.27	-0.29	-0.29	-0.04	-0.19

Table 4. Fourier series of annual radiation from sun in Jamshedpur

		0	1	2	3	4	5	6
yearly	T_0	188.5						
	Constant COS term		-22.73	-32.48	3.187	-11.47	10.05	-6.60
	Constant SIN term		26.67	-5.584	11.27	1.353	2.948	3.623
hottest	T_0	242.2						
	Constant COS term		-384.6	181.6	-33.36	-15.73	22.87	-21.19
	Constant SIN term		-19.31	15.64	-6.04	8.629	-7.86	-6.35

coldest	T_0	156.7						
	Constant COS term		-265.8	155	-48.21	-8.655	17.17	-6.444
	Constant SIN term		-24.95	27.76	-10	-7.665	10.3	-2.285

Tables 3 and 4 contain the coefficients of the Fourier series for temperature of air and radiation from sun fluctuation, respectively. These coefficients are specified for the warmest and coolest days of the year. The measured data of temperature of air and radiation from sun for the hottest and coldest days of the year were used to determine the best curve fit for computing these values. Radiation from sun fluctuation and temperature fluctuation at Jamshedpur for hottest summer day (17th June 2021), coldest winter day (28th December 2021) and yearly is taken as six-term harmonica.

The offered six harmonics are enough for capturing all of the measured data with an R^2 of close to 98%.

T_e	m	0	1	2	3	4	5	6
Dry sunlit surface	T_m	22.9330	12.6948	6.6336	2.3347	0.6191	0.7325	0.4186
	ψ_m		0.2702	0.2092	0.3029	1.3182	0.5120	0.7653
Wet sunlit surface	T_m	17.3253	2.5029	1.2818	0.4594	0.1264	0.1381	0.0857
	ψ_m		0.2942	0.2142	0.3164	1.3838	0.5067	0.8075
Dry sheltered surface	T_m	16.7202	2.9380	0.4414	0.4364	0.3505	0.0650	0.2047
	ψ_m		0.9554	0.6787	0.7577	1.0033	0.8652	1.3423
Wet sheltered surface	T_m	16.1368	0.6571	0.0987	0.0976	0.0784	0.0145	0.0457
	ψ_m		0.9554	0.6787	0.7577	1.0034	0.8652	1.3423

Table 5. Fourier analysis of effective temperature (T_e) fluctuation for hottest summer day (17th June 2021) in Jamshedpur (India) for various surface conditions

T_e	m	0	1	2	3	4	5	6
Dry sunlit surface	T_m	43.3729	19.214	6.9999	1.6174	0.7078	1.2987	0.9805

ISSN 2063-5346

	ψ_m		0.2879	0.1930	0.1297	0.3372	0.4185	0.4448
Wet sunlit surface	T_m	21.7872	3.8192	1.3333	0.3183	0.1358	0.2596	0.1913
	ψ_m		0.3184	0.2117	0.1229	0.3091	0.4289	0.4675
Dry sheltered surface	T_m	33.7702	5.6644	0.7945	0.2828	0.1169	0.3535	0.4806
	ψ_m		0.9757	1.1424	0.1074	1.1750	0.6570	0.3613
Wet sheltered surface	T_m	19.9501	1.2668	0.1777	0.0632	0.0261	0.0790	0.0393
	ψ_m		0.9758	1.1424	0.1074	1.1749	0.6570	1.3121

Table 6. Fourier analysis of effective temperature (T_e) fluctuation for coldest winter day (28th December 2021) in Jamshedpur (India) for various surface conditions

Table 7. Fourier study of annual effective temperature (T_e) change in Jamshedpur, India, under different surface conditions.

T_e	m	0	1	2	3	4	5	6
Dry sunlit surface	T_m	31.0238	6.1044	3.8583	0.8184	1.2070	0.8557	0.7684
	ψ_m		0.2287	0.3037	1.1669	0.7017	0.0565	0.0223
Wet sunlit surface	T_m	19.0941	1.3231	0.8210	0.1716	0.2601	0.1788	0.1633
	ψ_m		0.2097	0.3106	1.1119	0.7433	0.0816	0.0050
Dry sheltered surface	T_m	23.5503	4.8570	2.5692	0.5424	0.9548	0.4849	0.5220
	ψ_m		0.0673	0.3714	0.5989	1.0596	0.3476	0.2449
Wet sheltered surface	T_m	17.6644	1.0863	0.5746	0.1213	0.2135	0.1084	0.1168
	ψ_m		0.0673	0.3714	0.5989	1.0587	0.3476	0.2449

Table 5, table 6, and table 7 shows the coefficient of Fourier series for hottest summer day, coldest winter day and yearly fluctuation of effective temperature of various soil surface condition.

The fluctuations in temperature of air, radiation from sun, and speed of wind during the hottest summer day and coldest winter days are depicted in Figure 4. In Figure 4(a), can be seen hourly fluctuations in temperature of air, radiation from sun, and speed of wind on the hottest summer day and coldest winter day. The graph shows that the highest temperature of air for the summer day occurs at 3:00 PM, while the lowest temperature occurs at 5:00 AM. Similarly, for the winter day, the

highest temperature occurs at 3:00 PM, and the lowest temperature occurs at 6:00 AM. This information helps in understanding the patterns and trends of these variables during the day. The intensity of radiation from sun is displayed in Figure 4(b), which indicates that it reaches its peak at 2:00 PM on hottest summer day and coldest winter day. The fluctuation of speed of wind throughout the day on hottest summer day and coldest winter day is illustrated in Figure 4(c). During the night, radiation is zero and with the sunrise, the solar intensity is increasing and getting highest at 2 PM. After 2 PM the radiation from sun is decreasing. There is a fluctuation in the speed of wind throughout the day, its highest value occurs during the day and its lowest value occurs at night. Due to very less value of fluctuation of speed of wind it can be taken as constant value. Mean value of speed of wind is taken as Constant value, which is 2.17m/s.

Section A-Research Paper
ISSN 2063-5346

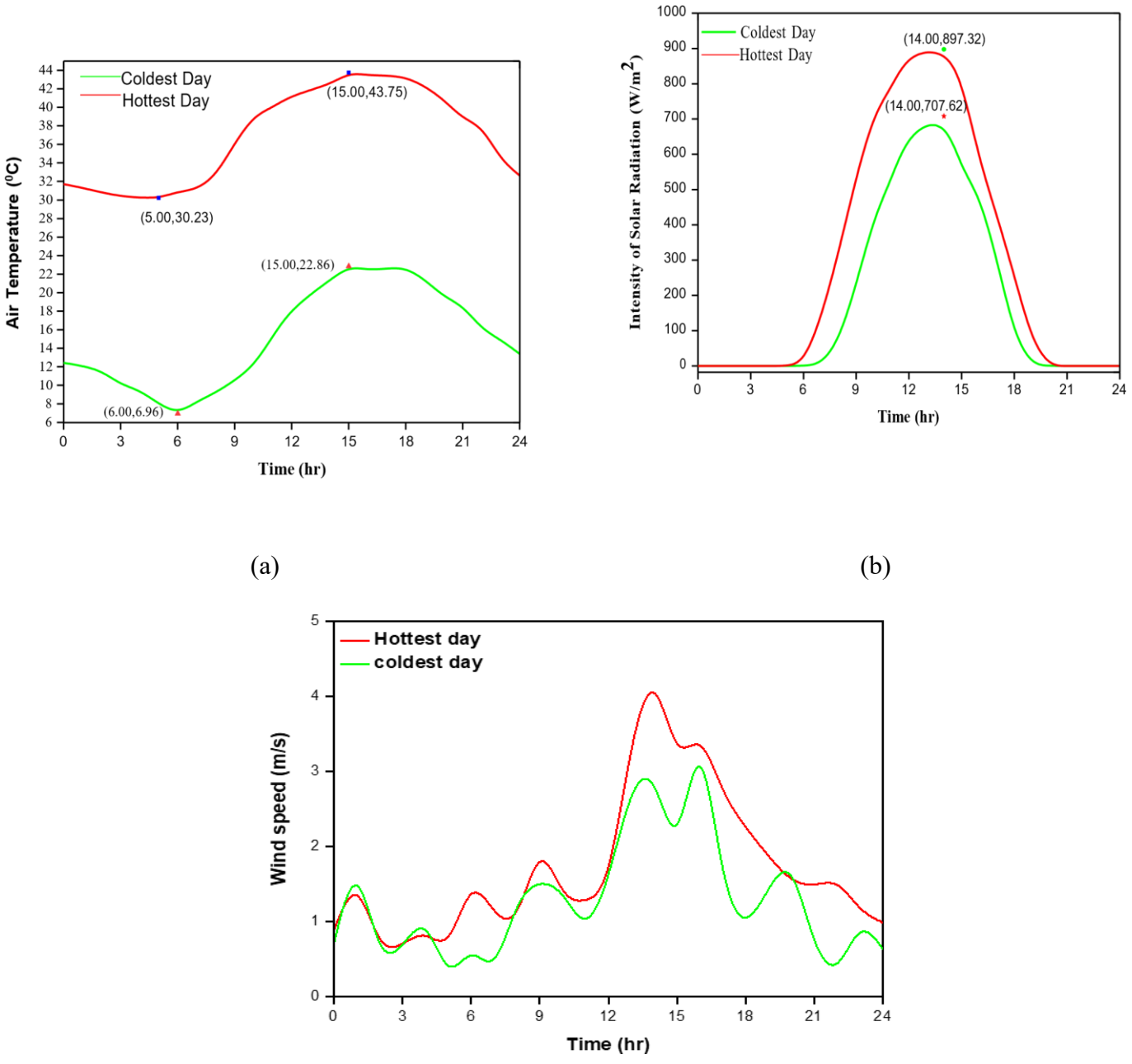

(a) (b)

(c)

Figure 4. Metrological data for hottest summer day, 17 June 2021 and coldest winter day, 28 December 2021 in Jamshedpur, India (a) Ambient temperature of air, (b) Radiation from sun intensity, and (c) Speed of wind

Figure 5 shows the effective temperature (T_e) of hottest summer and coldest winter day for different soil conditions. For different soil conditions, Figure 5 shows the effective temperature
(T_e) of the hottest summer and coldest

hand, for dry and wet sheltered conditions, temperature is dominant. Additionally, as the highest effective temperature is achieved per Figure 4(a), the highest temperature of near 03:00 PM as direct radiation from sun air is achieved at 03:00 PM. is negligible and the effect of surrounding

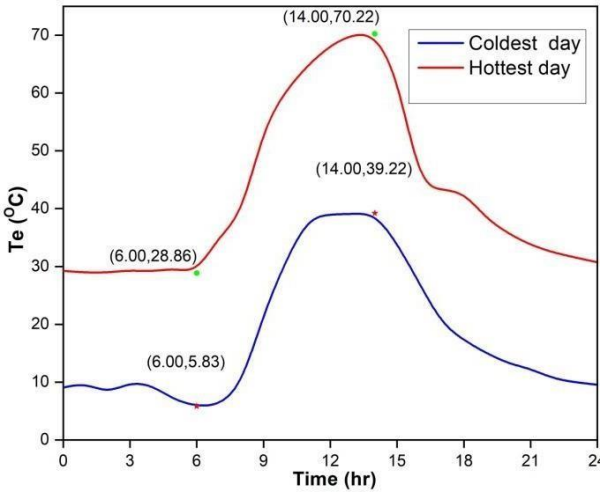

(a)

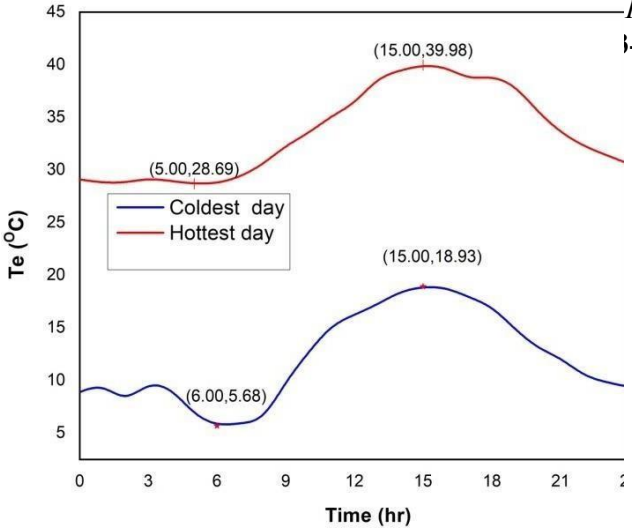

(b)

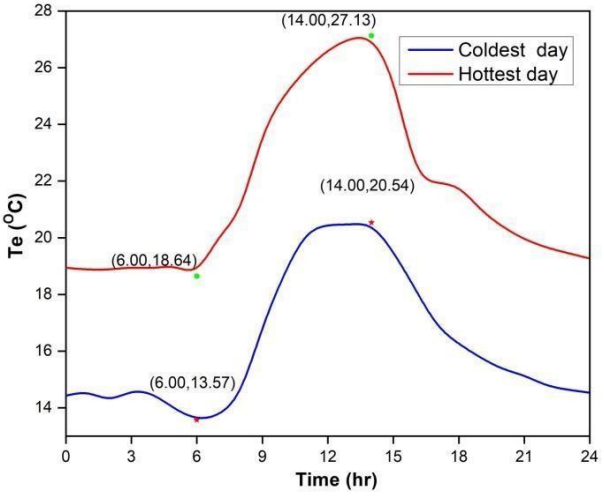

(c)

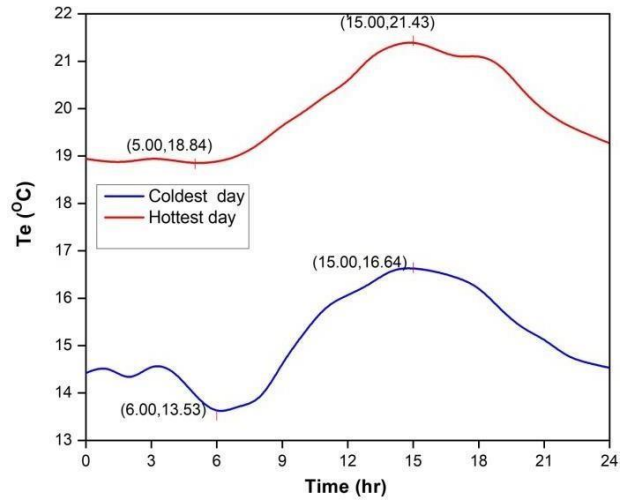

(d)

winter days. The highest effective temperature for both dry and wet sunlit conditions is achieved near 02:00 PM on both the hottest summer and coldest winter days because that's when the sunlit surface has highest solar intensity. On the other Figure 6 is the effective temperature for the year 2021 for different soil conditions. Soil receives highest radiation from sun and lowest evaporation in sunlit condition which in result highest temperature fluctuation. Lowest temperature fluctuation in wet sheltered condition due to lowest radiation from sun and highest evaporation. The sunlit soil condition has the highest amplitude fluctuation of temperature whereas the wet soil condition has lowest amplitude fluctuation of temperature.

Section A-Research Paper
ISSN 2063-5346

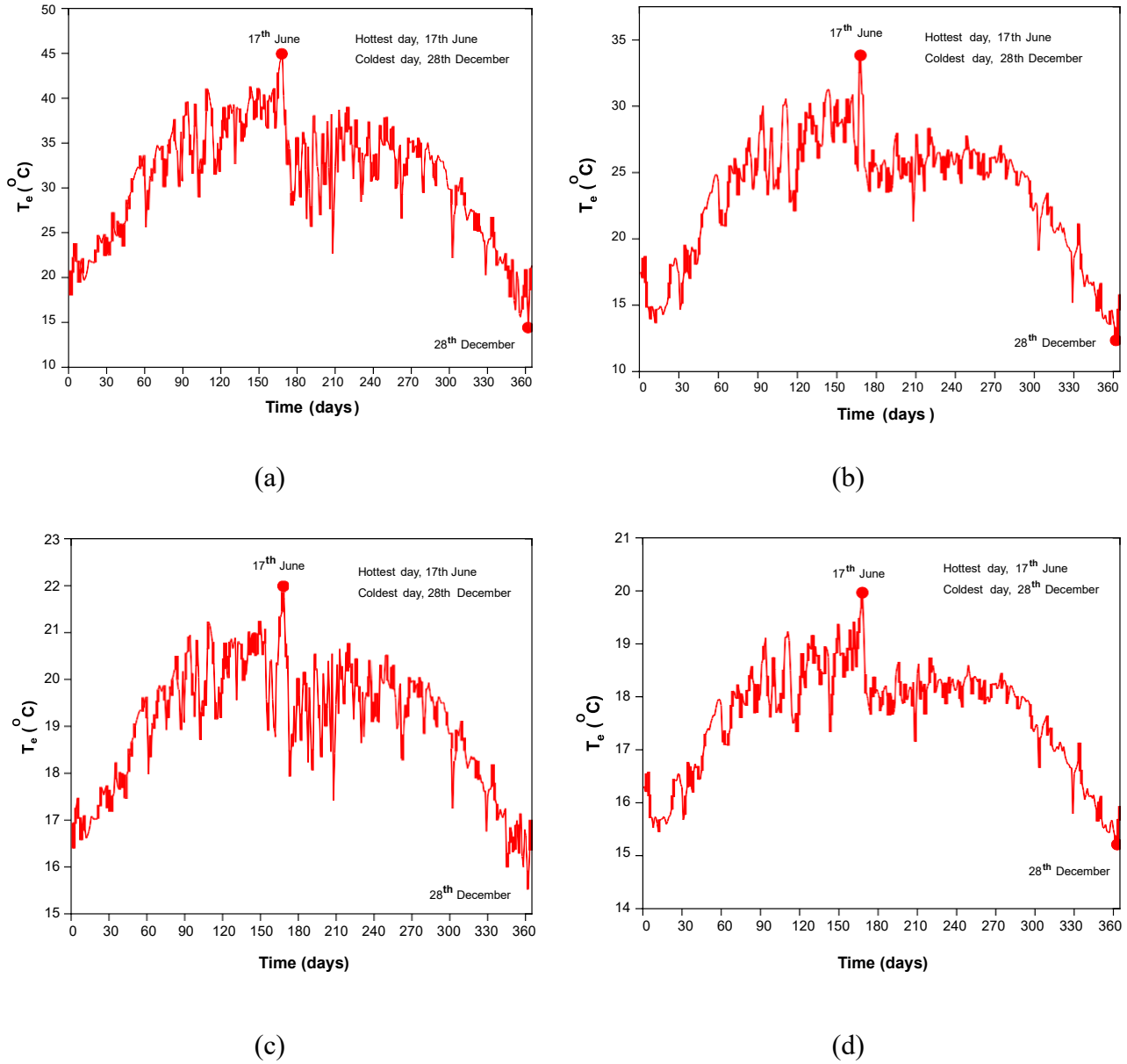

Figure 6. Daily T_e fluctuation for (a) Dry Sunlit (b) Dry Sheltered (c) Wet Sunlit (d) Wet Sheltered

5.1 Validation with CFD Results

The validation between the experimental and CFD model outcomes for soil temperature is satisfying. This suggests that the CFD model precisely replicates the transmission of heat mechanism in the soil system. In order to cover a broad range of soil temperature and facilitate comprehensive comparison, selected cold winter days (December 5) and hot summer days (May 5) from 2021 to represent the two extreme weather conditions. For validation with experimental results, In CFD modeling for hot summer days, two layers is used: up to a depth of 0.5 m, dry soil; below 0.5 m, soil with a water content of 20%; both layers are conjugate to one another. In cold winter day soil properties in CFD model is soil with water content is 20% throughout the depth as of experimental result. A 24-hour period on each of these dates was chosen for comparison of the experimental temperature data and CFD model results, with time measured from 12 o'clock midnight. The hourly fluctuation of soil temperature on both summer and winter days was simulated using ANSYS 19.0 (CFD), and compared with measured experimental values. The results indicate a reasonable agreement between the two, with the percentage error with respect to the experimental values being recorded. Figure 7 displays the hourly temperature fluctuation over time for both experimental and CFD model data.Temperature values estimated numerically using ANSYS 19.0 (CFD) for periods of 5, 10, 15, and 20 hours on December 5, 2021 and May 5, 2021 are compared to those obtained experimentally in Figures 7 (a) and 7 (b). The findings show that the computational and experimental numerical values coincide quite well.

Figure 8(a) compares soil temperature between experimental and CFD simulation results for five different days throughout the year: February 10th, April 10th, June 10th, August 10th, and December 10th. The data indicates that the soil temperature values derived from the CFD

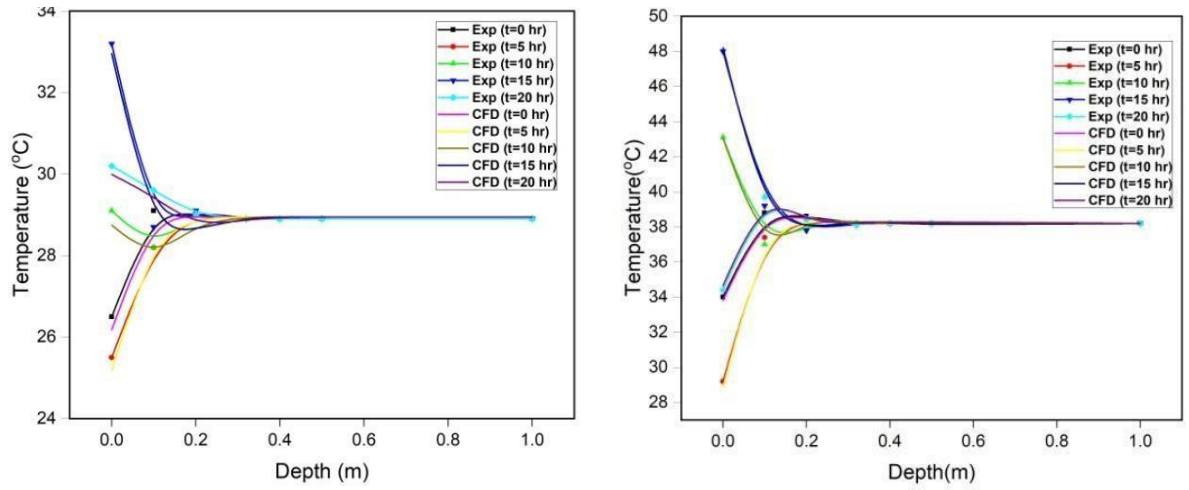

(a) (b)

Figures 7. The experimental and simulation (hourly on day) fluctuation of soil temperature with depth, (a) for December 5, 2021, (b) for May 5, 2021.

tool for predicting soil temperature dynamics, which has implications for various applications, such as agriculture, ecology, and climate science.

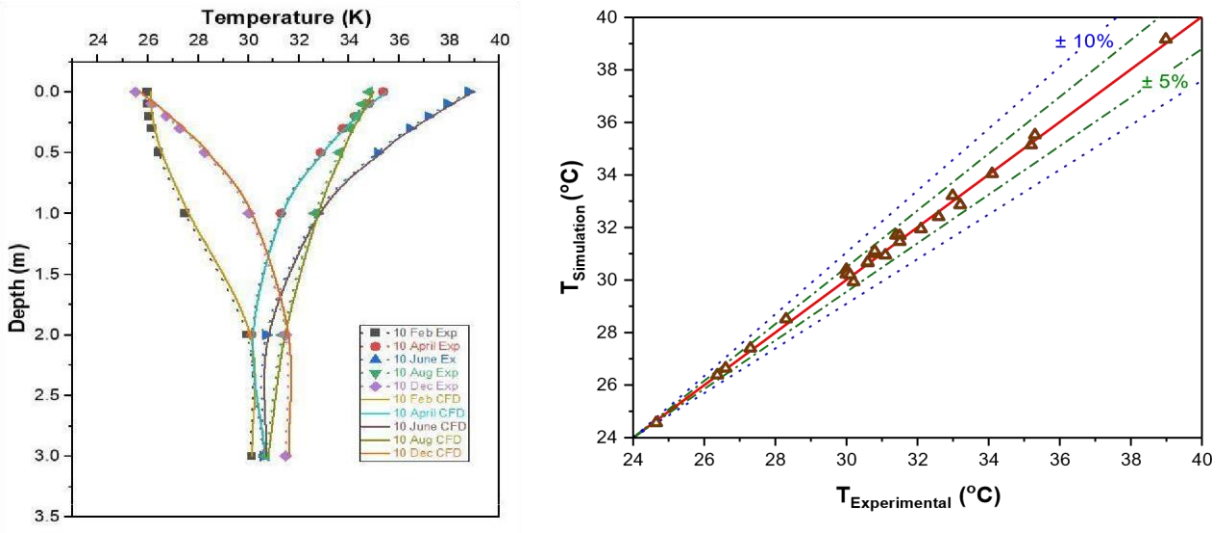

(a) (b)

Figure 8. (a) Experimental and CFD simulations of the temperature profile in the earth throughout the year on different day, (**b**) the consistency of the model with the experimental and simulation results.

simulation are consistent with the experimental results, indicating that the CFD model accurately represents the investigated actual system. Figure 8 (b), which shows the consistency between the experimental and simulation results. The figure shows that most of the results fall within a 5% error band, which indicates a high level of agreement between the two sets of data (experimental and simulated). Additionally, it notes that there is only one result that falls outside of the 5% error band, but that this result still falls within the less stringent 10% error band. This suggests that the experimental and simulation results are close to each other and that both sets of data (experimental and simulated) validate each other. These findings are important because they suggest that the CFD simulation model is a reliable

ISSN 2063-5346

Figure 9 shows the hottest summer day soil temperature fluctuation. The daily amplitude fluctuation of soil is highest at surface while gradually decreases with depth and become constant at 0.2m. The dry sunlit and sheltered temperature at depth below 0.2m is about 43°C and 34°C whereas wet temperature is about 21.8°C and 13°C. The amplitude difference is higher in sunlit soil surface as compared to wet soil surface.

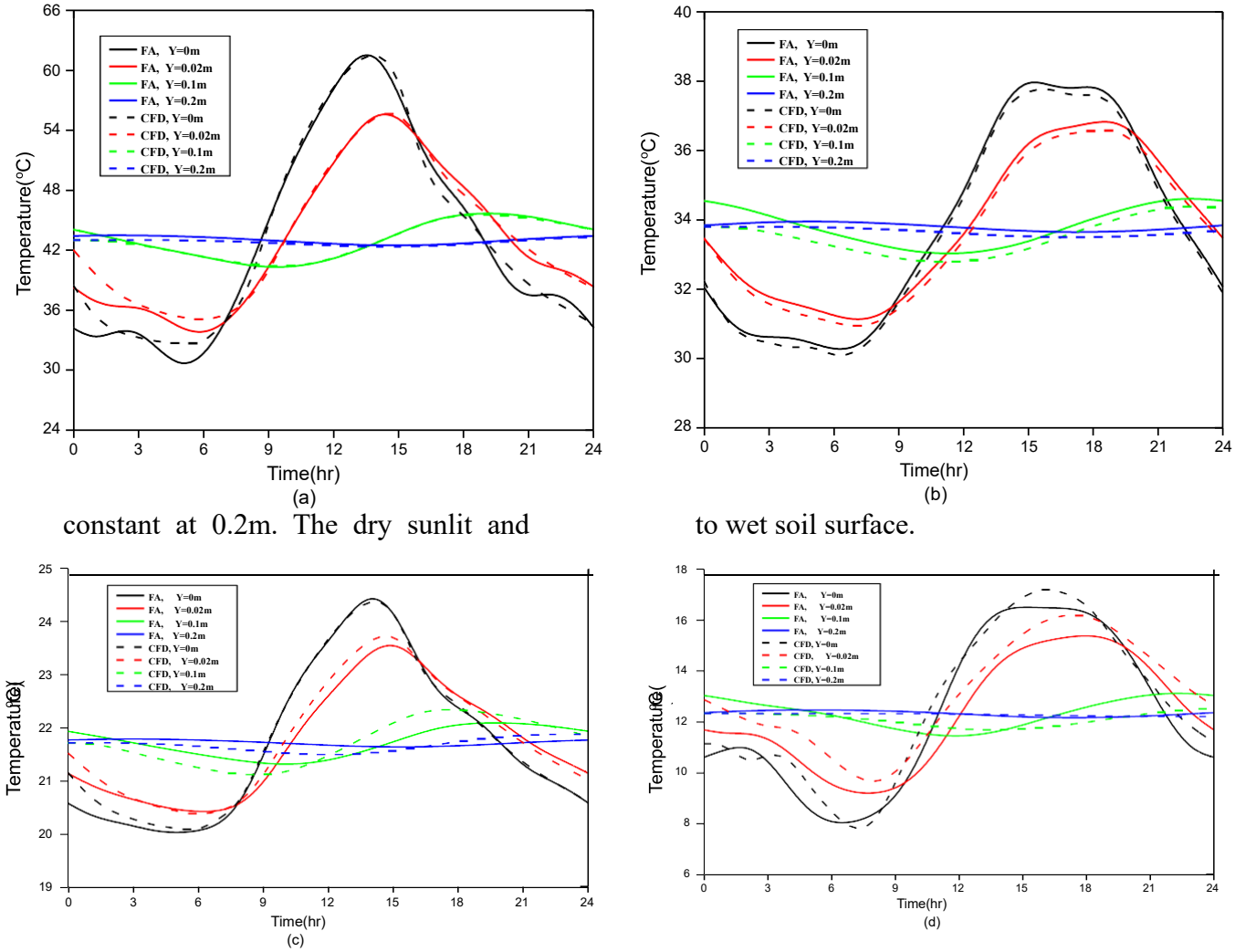

Figure 9. Hottest summer day temperature fluctuation in 24 hours, (a) Dry Sunlit, (b) Dry Sheltered, (c) Wet Sunlit, and (d) Wet Sheltered

Figure 10 shows the temperature contour for different soil conditions at hottest time which is 2PM for dry and wet sunlit condition and 3PM for dry and wet sheltered condition on hottest summer day. The red color shows the upper surface temperature is higher while temperature decreases with an increase of depth and remains constant after 0.2m.

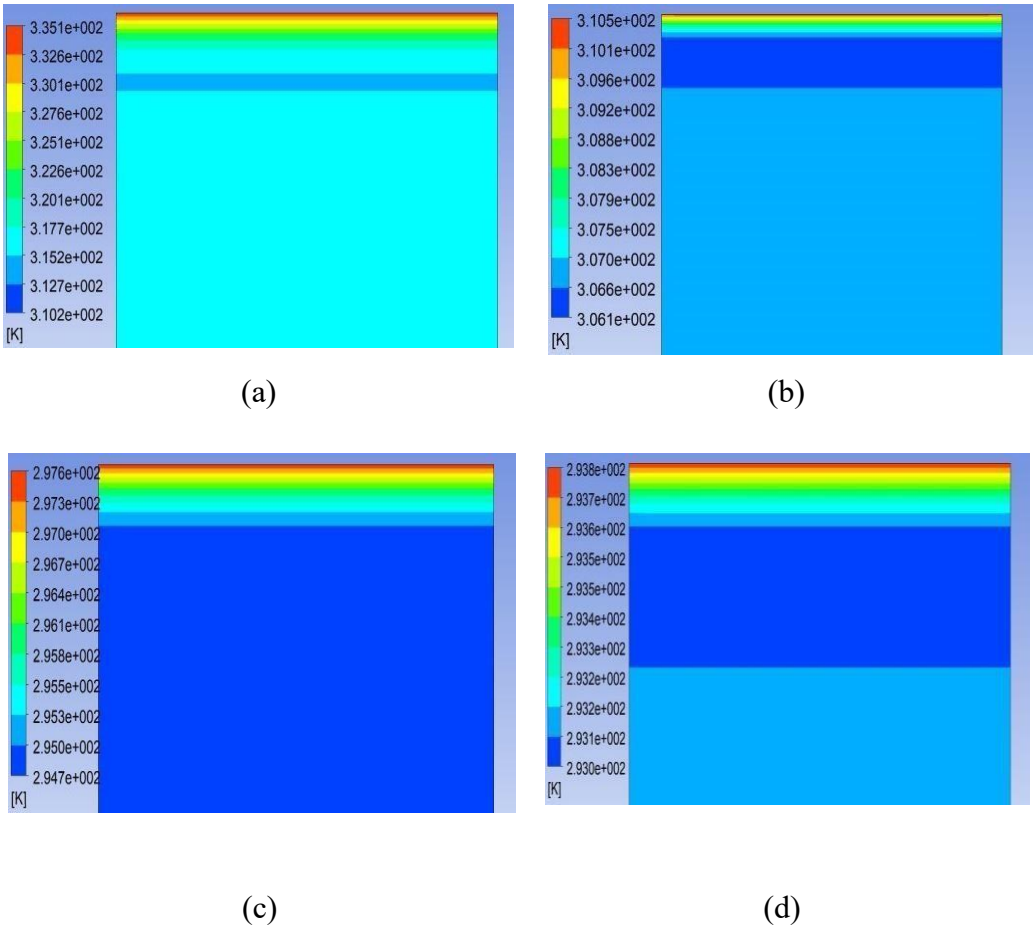

Figure 10. Hottest summer day temperature contour for, (a) Dry Sunlit, (b) Dry Sheltered, (c) Wet Sunlit, and (d) Wet Sheltered

Figure 11 shows the coldest winter day of soil temperature fluctuation. For coldest day the daily amplitude fluctuation is similar to hottest summer day amplitude fluctuation, which is highest at surface while gradually decreases with depth and constant at 0.2m.

The dry sunlit and sheltered consist temperature at depth below 0.2m as about 19°C and 12.5°C whereas wet temperature is about 16.4°C and 15.1°C. The amplitude difference is higher in sunlit soil surface as compare to wet soil surface.

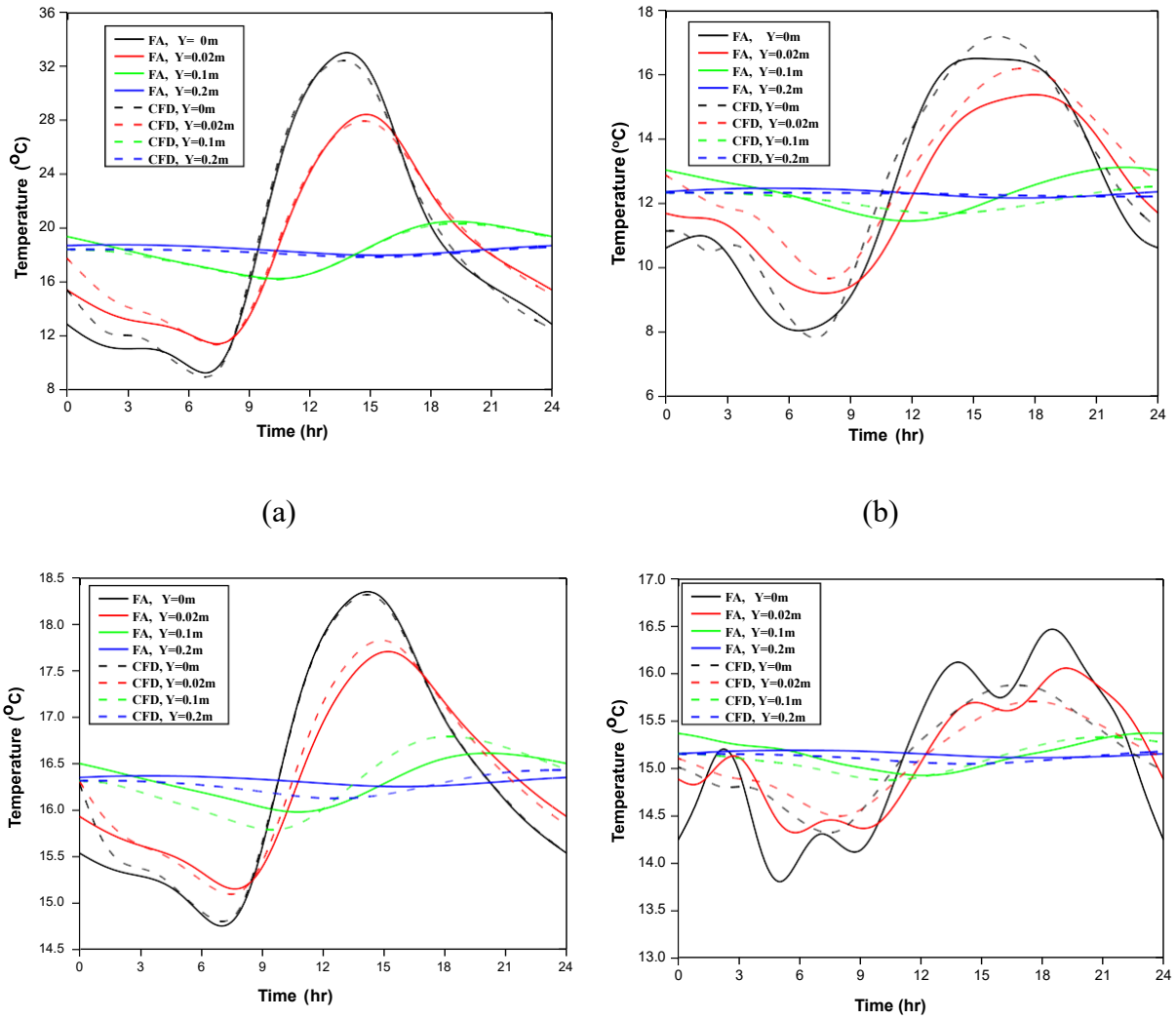

Figure 11. Coldest day temperature fluctuation in 24 hours, (a) Dry Sunlit, (b) Dry Sheltered, (c) Wet Sunlit, and (d) Wet Sheltered

Figure 12 show the temperature time 6AM for coldest winter day. The blue contour of coldest temperature during the color shows the upper surface temperature is entire day. For different soil conditions the lower and increases with depth and remains coldest temperature measured at coldest constant after 0.2m.

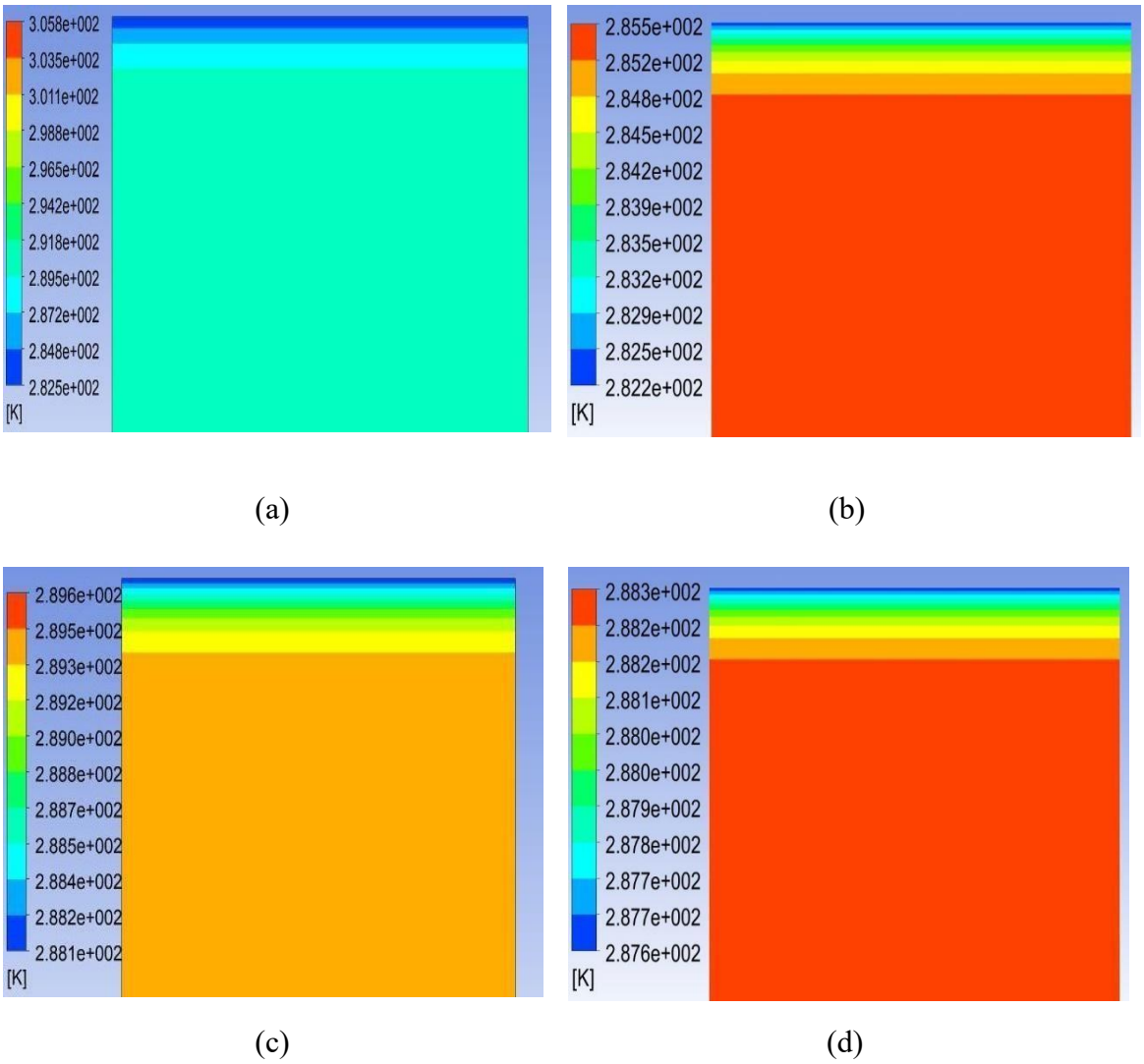

Figure 12. Coldest day temperature contour for, (a) Dry Sunlit, (b) Dry Sheltered, (c) Wet Sunlit, and (d) Wet Sheltered

Tables 3 and 4 present the six-term harmonic Fourier coefficient term for yearly temperature fluctuation over a time period of ω=2* π/365, as investigated in this study. Figure 13 depicts the soil temperature fluctuation under various soil conditions throughout the year. The outcomes suggest that the temperature fluctuation at a depth of about 4m remains consistent, as indicated by

both the theoretical and CFD simulation results.

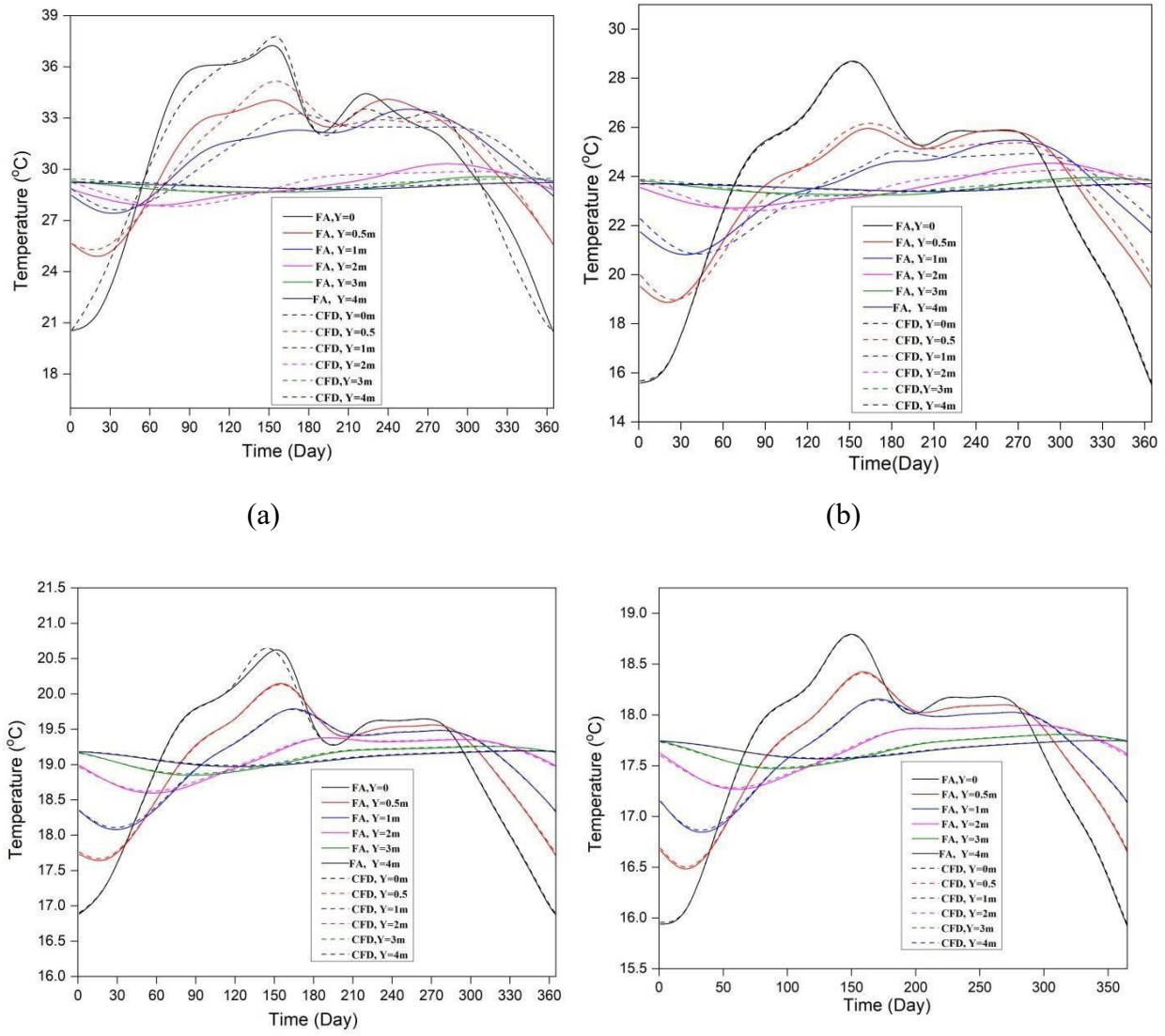

Figure 13. Yearly temperature Fluctuation in 2021, (a) Dry Sunlit, (b) Dry Sheltered, (c) Wet Sunlit, and (d) Wet Sheltered

Conclusions

In this investigation, the finite volume method (CFD) and Fourier temperature profile as a function of time and depth at any site. The study also highlights fluctuation in temperature of soil in the model's capability to assess the magnitude of heat fluxes occurring at the earth's surface. experimentally determined soil temperature, or sink for earth-coupled heat pumps. Furthermore, with knowledge of the climate conditions, the model can predict the earth numerical methods were employed to study the Jamshedpur, Jharkhand, India. The results indicate that the CFD model aligns with the

(1) The amplitude of diurnal temperature fluctuation extends to a depth of 4 m.
(2) The depth wise amplitude of soil temperature for wet surface has less fluctuation as compare to sunlit soil surface.
(3) The wet sheltered surface has lowest soil temperature in both diurnal and annual among of other soil surface condition.
(4) For hottest summer day, the highest temperature for diurnal fluctuation of soil temperature on the soil surface is achieved near 2 PM for all surface condition. While for coldest winter day, highest temperature is achieved near 2PM for sunlit condition and 3PM for sheltered condition.
(5) For hottest summer day, the lowest temperature for diurnal fluctuation of soil temperature on the soil surface is achieved near 6AM for sunlit condition and 5AM for sheltered condition. While for coldest winter day, lowest temperature is achieved near 6AM for all surface condition.
(6) Experimental and simulated results are close to each other and validate each other, with only one result outside of the 5% error band.

The findings of this investigation could have significant implications for the design and optimization of earth-coupled heat pump systems, which rely on the subsurface as a heat source or sink. The use of CFD modelling and Fourier analysis can improve our understanding of the thermal behavior of the subsurface, which can lead to more efficient and sustainable energy systems. The study also demonstrates the potential of numerical modelling techniques to provide accurate predictions of earth temperature profiles, which can be valuable information for a range of applications, including building design, agriculture, and geothermal energy.

Authors' contribution

Gajendra Kumar developed the theoretical work, wrote the computer code, and drafted the manuscript. Ram Vinoy Sharma participated as a research mentor, checked the paper and data analysis, and Radha Krishna Prasad scrutinized the manuscript.

Funding: Not applicable.

Conflict of interest: The authors declare that they have no conflict of interest. **References**

[1] T. Kusuda and P. R. Achenbach, "Earth temperature and thermal diffusivity at selected stations in the United States," National Bureau of Standards Gaithersburg MD, 1965.

[2] A. K. Khatry, M. S. Sodha, and M. A.

S. Malik, "Periodic fluctuation of earth temperature with depth," *Solar Energy*, vol. 20, no. 5, pp. 425–427, 1978.

[3] G. Mihalakakou, M. Santamouris, J. O. Lewis, and D. N. Asimakopoulos, "On the application of the energy balance equation to predict earth temperature profiles," *Solar Energy*, vol. 60, no. 3– 4, pp. 181–190, 1997.

[4] W. R. Herb, B. Janke, O. Mohseni, and H. G. Stefan, "Earth surface temperature simulation for different land covers," *J Hydrol (Amst)*, vol. 356, no. 3–4, pp. 327–343, 2008.

[5] G. Mihalakakou, M. Santamouris, D. Asimakopoulos, and A. Argiriou, "On the earth temperature below buildings," *Solar energy*, vol. 55, no. 5, pp. 355– 362, 1995.

[6] M. Ouzzane, P. Eslami-Nejad, Z. temperature fluctuation," *Geothermal* Aidoun, and L. Lamarche, "Analysis of *Energy*, vol. 5, no. 1, pp. 1–10, 2017. the convective heat exchange effect on the undisturbed earth temperature," *Solar Energy*, vol. 108, pp. 340–347, 2014, doi: https://doi.org/10.1016/j.solener.2014.07.015.

[7] J. P. D. Charpin, T. G. Myers, A. D. pp. 11–15, 1991. Fitt, Y. Ballim, and A. Patini, "Modeling surface heat exchanges from a concrete block into the environment,"

[8] P. J. Cleall, J. J. Muñoz-Criollo, and S. exchangers," *Renew Energy*, vol. 103, W. Rees, "Analytical solutions for earth pp. 295–307, 2017. temperature profiles and stored energy using meteorological data," *Transp Porous Media*, vol. 106, pp. 181–199, 2015. undisturbed earth temperature,"

[9] F. Droulia, S. Lykoudis, I. Tsiros, N. *Geothermics*, vol. 53, pp. 379–384, Alvertos, E. Akylas, and I. Garofalakis, "Earth temperature estimations using Harris, simplified analytical *Energy*, "The generation of temperature profiles for

[13] S. D. Wullschleger, J. E. Cahoon, J. A. Ferguson, and D. M. Oosterhuis, "SURFTEMP: Simulation of soil surface temperature using the energy balance equation," *Journal of agronomic education*, vol. 20, no. 1,

[14] M. Chalhoub, M. Bernier, Y. Coquet, and M. Philippe, "A simple heat and moisture transfer model to predict earth temperature for shallow earth heat exchangers," *Renew Energy*, vol. 103, pp. 295–307, 2017.

[15] M. Ouzzane, P. Eslami-Nejad, M. Badache, and Z. Aidoun, "New correlations for the prediction of the 2015.

[16] A. A. Al-Temeemi and D. J. and semi- empirical approaches," *Solar* subsurface vol. 83, no. 2, pp. 211–219, 2009. Kuwait,"

[10] T. R. H. Holmes, T. J. Jackson, R. H. Basara, "An assessment of surface soil temperature products from numerical weather prediction models using earth-based precipitation measurements," *Water Resour Res*, vol. 48, no. 2, 2012.

[11] T. Yilmaz, A. Oezbek, A. Yilmaz, and O. Bueyuekalaca, "INFLUENCE OF UPPER LAYER PROPERTIES ON THE EARTH TEMPERATURE DISTRIBUTION.," *Isi Bilimi ve Teknigi Dergisi/Journal of Thermal Science & Technology*, vol. 29, no. 2, 2009.

[12] R. K. Singh and R. V. Sharma, "Numerical analysis for earth *Environ*, vol. 16, no. 3, pp. 183–192, 1981.

[20] Y. Zheng *et al.*, "Encapsulated phase change materials for energy storage – Characterization by calorimetry," *Solar Energy*, vol. 87, no. 1, pp. 117–126, Jan. 2013, doi: 10.1016/J.SOLENER.2012.10.003.

[21] O. Ozgener, L. Ozgener, and J. W. Tester, "A practical approach to predict soil temperature fluctuations for geothermal (earth) heat exchangers applications," *Int J Heat Mass Transf*, vol. 62, pp. 473–480, 2013.

[22] R. Kumar Singh and R. V Sharma, "Mathematical Investigation of Soil Temperature Fluctuation for Geothermal Applications," *International Journal of Energy Build*, vol. 33, no. 8, pp. 837–841, 2001. Reichle, and J. B. Running, "A daily soil temperature model based on temperature of air and for continental applications," *Clim Res*, vol. 2, no. 3, pp. 183–191, 1993.

[17] D. Zheng, E. R. Hunt Jr, and S. W.

[18] H. Tabari, A.-A. Sabziparvar, and M. Ahmadi, "Comparison of artificial neural network and multivariate linear regression methods for estimation of daily soil temperature in an arid region," *Meteorology and Atmospheric Physics*, vol. 110, pp. 135–142, 2011.

[19] S. S. Bharadwaj and N. K. Bansal, "Temperature distribution inside earth for various surface conditions," *Build*

Engineering, vol. 30, no. 10, pp. 1609–1614, 2017.

[23] H. S. Carslaw and J. C. Jaeger, "Conduction of heat in solids," *Conduction of heat in solids*, 1947.

.

[24] M. Krarti, C. Lopez-Alonzo, D. E. Claridge, and J. F. Kreider, "Analytical model to predict annual soil surface temperature fluctuation," 1995.

[25] W. M. Kays and M. E. Crawford, "Convective Heat and Mass Transfer McGraw-Hill," *New York*, pp. 255– 282, 1993.

[26] H. L. Penman, "Vegetation and hydrology," *Soil Sci*, vol. 96, no. 5, p. 357, 1963.

[27] M. Ş. İŞ, "DETERMINATION OF EARTH TEMPERATURE IN ADANA".

[28] M. Krarti, C. Lopez-Alonzo, D. E. Claridge, and J. F. Kreider, "Analytical Model to Predict Annual Soil Surface Temperature Fluctuation," *J Sol Energy Eng*, vol. 117, no. 2, pp. 91–99, May 1995, doi: 10.1115/1.2870881